



Contents lists available at ScienceDirect

Journal of the European Ceramic Society

journal homepage: [www.elsevier.com/locate/jeurceramsoc](http://www.elsevier.com/locate/jeurceramsoc)

Short communication

# Enhancement of densification and microwave dielectric properties in LiF ceramics via a cold sintering and post-annealing process

Bing Liu<sup>a</sup>, Lei Li<sup>b</sup>, Kai Xin Song<sup>a,d,\*</sup>, Min Min Mao<sup>a</sup>, Zhilun Lu<sup>d</sup>, Ge Wang<sup>d</sup>, Linhao Li<sup>d</sup>, Dawei Wang<sup>d</sup>, Di Zhou<sup>e</sup>, Antonio Feteira<sup>c,\*\*</sup>, Ian M. Reaney<sup>d,\*\*</sup>

<sup>a</sup> College of Electronic Information, Hangzhou Dianzi University, Hangzhou 310018, China<sup>b</sup> School of Materials Science and Engineering, Zhejiang University, Hangzhou 310027, China<sup>c</sup> Christian Doppler Lab on Advanced Ferroic Oxides, Materials and Engineering Research Institute, Sheffield Hallam University, Sheffield, S1 1WB, UK<sup>d</sup> Department of Materials Science and Engineering, University of Sheffield, Sheffield, S1 3JD, UK<sup>e</sup> Electronic Materials Research Laboratory, Key Laboratory of the Ministry of Education & International Center for Dielectric Research, Xi'an Jiaotong University, Xi'an 710049, China

## ARTICLE INFO

## Keywords:

LiF  
Cold sintering  
Microwave dielectric properties  
Densification

## ABSTRACT

LiF is a low-firing fluoride with excellent microwave dielectric properties, however densification of LiF ceramics is challenging owing to their low surface free energy. In this study, a cold sintering process (150 °C, 250 MPa, 60 min) was employed to pre-densify LiF ceramics to 78 % relative density. Post-annealing treatments between 650 °C and 800 °C led to significant grain growth which was accompanied by an increase in relative density to 92 %. The microwave quality factor ( $Qf$ ) increased with increasing annealing temperature to a maximum of 110,800 GHz at 800 °C, 1.5 times higher than the value obtained via conventional sintering (78,800 GHz), with relative permittivity  $\epsilon_r = 8.2$  and temperature coefficient of resonant frequency,  $\tau_f = -135$  ppm/°C. Such high values of  $Qf$  and its compatibility with Ag electrode suggest that cold sintered LiF has great potential as a component or additive in low temperature co-fired ceramic formulations.

## 1. Introduction

Over the past decades, with the rapid developments of wireless communications, microwave (MW) dielectric ceramics have been widely investigated as critical components of passive microwave devices such as substrates, resonators and filters, [1,2]. Furthermore, to satisfy the demands of miniaturization and multifunction of modern electronic devices, low temperature co-fired ceramic (LTCC) technology has attracted much attention from both scientific and industrial stakeholders. For LTCC applications, the densification temperature of the microwave dielectric ceramics should be lower than the melting temperatures of metallic electrodes such as Ag (~961 °C) [3–6]. The sintering temperature of most ceramics (>1200 °C) clearly exceeds the melting temperature of the electrodes, thereby precluding co-firing. The most common strategy to reduce the sintering temperature is the addition of a low melting point component [4,4,5,6]. Unfortunately, this leads to the formation of secondary phases with inferior dielectric performance. Hence the reduction of sintering temperature is accomplished

at the expense of MW quality factor.

An alternative to meeting LTCC requirements involves the search for dielectric ceramics with intrinsically low sintering temperature. Among them, lithium-based oxides have been explored, such as  $\text{Li}_2\text{Mg}_3\text{ZnO}_6$ ,  $\text{Li}_2\text{MgGeO}_4$  and  $\text{Li}_2\text{WO}_4$ , with low sintering temperature and good dielectric performance. [7–9] With the success of lithium based oxides, researchers expanded the search for new dielectric ceramics to fluorides and oxyfluorides with many materials exhibiting ideal properties for MW applications [10], e.g. Fang et al. reported the synthesis of fluorine-containing  $\text{Li}_5\text{Ti}_2\text{O}_6\text{F}$  ceramics with excellent MW dielectric performance ( $\epsilon_r = 19.6$ ,  $Qf = 79,500$  GHz, and  $\tau_f = -29.6$  ppm/°C) [11].

LiF has been widely applied as an effective sintering additive or flux in many ceramic formulations but it was not until 2019 that Lei et al. first reported the synthesis of LiF ceramics via conventional sintering and their microwave dielectric properties,  $\epsilon_r = 8.02$ ,  $Qf = 73,880$  GHz, and  $\tau_f = -117.7$  ppm/°C [12]. However, Geyer et al. reported a much higher  $Qf$  value (192,400 GHz) for LiF single crystals [13]. According to Lei et al., the disparity in  $Qf$  with single crystal arises mainly from the

\* Corresponding author at: College of Electronic Information, Hangzhou Dianzi University, Hangzhou 310018, China.

\*\* Corresponding authors.

E-mail addresses: [kxsong@hdu.edu.cn](mailto:kxsong@hdu.edu.cn) (K.X. Song), [A.Feteira@shu.ac.uk](mailto:A.Feteira@shu.ac.uk) (A. Feteira), [i.m.reaney@sheffield.ac.uk](mailto:i.m.reaney@sheffield.ac.uk) (I.M. Reaney).

<https://doi.org/10.1016/j.jeurceramsoc.2020.09.073>

Received 24 July 2020; Received in revised form 15 September 2020; Accepted 30 September 2020

Available online 4 October 2020

0955-2219/© 2020 Elsevier Ltd. All rights reserved.

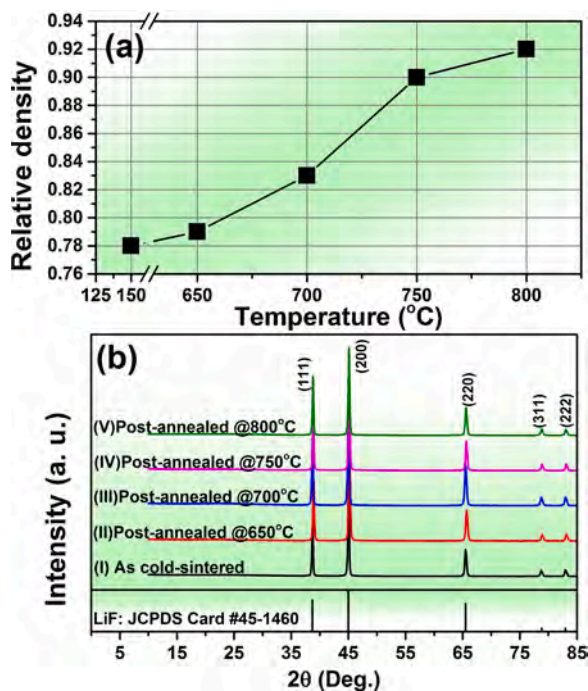


Fig. 1. (a) Relative density and (b) room-temperature XRD data of the cold-sintered and subsequently annealed LiF ceramics.

difficulty in densifying LiF ceramics which remain porous after conventional sintering [12].

Cold sintering (CS) is a novel sintering method which combines liquid-phase assisted and pressure-assisted sintering to help densify materials at low temperatures [14–16]. During CS, the powder is mixed with a solvent and then axially loaded to achieve densification. To accelerate the densification process, moderate temperatures (<200 °C) are applied. Many studies on CS have shown that densification generally occurs in materials with high solubility (mostly in water), such as NaCl (35.8 g/100 mL),  $H_3BO_3$  (4.77 g/100 mL),  $Li_2MoO_4$  (79.5 g/100 mL), etc. [17–20]. Although the mechanism of CS remains controversial, it is widely accepted that the dissolution and precipitation processes during CS plays a vital role in mass transport and densification [17–19]. Moreover, recent studies on the synthesis of vaterite and gypsum ceramics with relatively low solubility (~0.2 g/100 mL) have broadened the potential range of cold sintered materials [16,21]. Considering that LiF has a similar solubility (0.29 g/100 mL), we propose that CS is a promising approach to enhance the densification in LiF ceramics [20].

In this study therefore, LiF ceramics are pre-densified via the CS process followed by systematic post-annealing to optimize microwave properties. Furthermore, the chemical compatibility between LiF and Ag electrode is evaluated to reveal its potential for applications in LTCC technologies.

## 2. Experimental procedure

The starting LiF raw powder was supplied by Aladdin Chemical Reagent Co., LTD (99.99 %). Prior to weighing, LiF powder was dried at 150 °C for 12 h in a vacuum oven to remove potential moisture. The dried powder was then weighed and uniformly mixed with 10 wt.% of deionized water. The moist powder was placed into a metal die with a diameter of 12.7 mm and then pressed under a uniaxial pressure of 250 MPa. Along with the holding pressure, the die was heated from room temperature to 150 °C with a heating rate of 5 °C/min and then held for 60 min. Finally, the die was cooled to room temperature, and pellets with dimensions of 12.7 mm in diameter and 5 mm in height were successfully obtained. Further post-annealing of the as-prepared pellets

Table 1

The lattice parameters, reliability factors, and dielectric constants of the present ceramics.

Temperature (°C)	$a=b=c$ (Å)	$V$ (Å <sup>3</sup> )	$R_p\%$	$R_{wp}\%$	$\chi^2$	$\epsilon_r$	$\epsilon_{cor}$
150	4.02691 (45)	65.300 (13)	7.31	9.02	5.89	6.40	8.85
650	4.02903 (40)	65.404 (11)	5.33	7.23	4.04	6.45	8.76
700	4.02674 (41)	65.292 (11)	6.09	7.80	4.35	6.78	8.62
750	4.02847 (38)	65.377 (11)	5.87	7.61	4.38	7.67	8.9
800	4.02843 (40)	65.374 (11)	6.62	8.40	5.45	8.2	9.12

was carried out between 650 °C and 800 °C for 3 h with a heating rate of 5 °C/min and then cooled to room temperature within the furnace.

Relative density was calculated from the mass and volume of the sample. The volume was determined by measuring the thickness and area of the sample. The crystal structure and phase assemblage were determined by X-ray diffraction (XRD: RIGAKU D/max 2550/PC, Rigaku Co., Japan). Scanning electron microscopy (SEM) images of the polished and thermal-etched surfaces of LiF ceramics were obtained on a SIRION-100 (FEI Co., Eindhoven, Netherlands). The thermal etching was conducted at a temperature 25 °C lower than the annealing temperature for 30 min. The grain size distribution and the average grain size of the annealed samples were determined from the SEM images using an image analysis software (ImageJ, National Institute of Health, Bethesda, MD). A minimum of 100 measurements were performed for each average value reported. The MW dielectric properties were measured using a vector network analyzer (E8363B, Agilent Technologies Inc., Palo Alto, CA, USA). At last, the as cold sintered LiF ceramics were co-fired with Ag colloids (Ted Pella Inc., Redding, CA, USA) at 800 °C for 3 h to assess the chemical compatibility with electrodes. SEM image on the fracture surface of LiF-Ag composite was obtained, and the element distributions were recorded using an energy-dispersive spectrometer (EDS: X-Max 80 mm<sup>2</sup>, Oxford Instruments Co., Oxford, UK).

## 3. Results and discussion

After dry-pressing, the green density of ceramics was typically 40 %–60 % but as shown in Fig. 1(a) this is improved to ~78 % through cold sintering (CS) at 150 °C. This suggests that particle sliding in the presence of moisture and the slight solubility of LiF, leading to dissolution/precipitation, promotes densification during CS. However, according to Lei et al., the relative density of LiF ceramics via conventional sintering (800 °C) is ~90 %, higher than as cold-sintered samples [12]. To further promote the densification therefore, post-annealing of as cold-sintered samples is carried out at 650 °C, 700 °C, 750 °C, and 800 °C, respectively. As shown in Fig. 1(a), the relative density increases monotonously with increasing annealing temperature until a maximum value of ~92 % at 800 °C. Further increasing the annealing temperature to 850 °C leads to melting, and the corresponding results are excluded from the present study.

Fig. 1(b) shows the XRD patterns of LiF ceramics obtained at various processing temperatures. All diffraction patterns may be indexed based on the LiF crystal structure (JCPDS #45–1460) with no additional diffraction peaks related to the existence of secondary phases or structural phase transformations. Rietveld refinements of XRD patterns are carried out based on the  $Fm\bar{3}m$  LiF structure with the calculated and measured profiles shown in the supporting information, Figure S1. The calculated lattice parameters and the reliability factors are listed in Table 1. The CS process and subsequent annealing have little effect on phase purity, crystal structure or lattice parameters.

SEM images are collected from polished and thermally etched



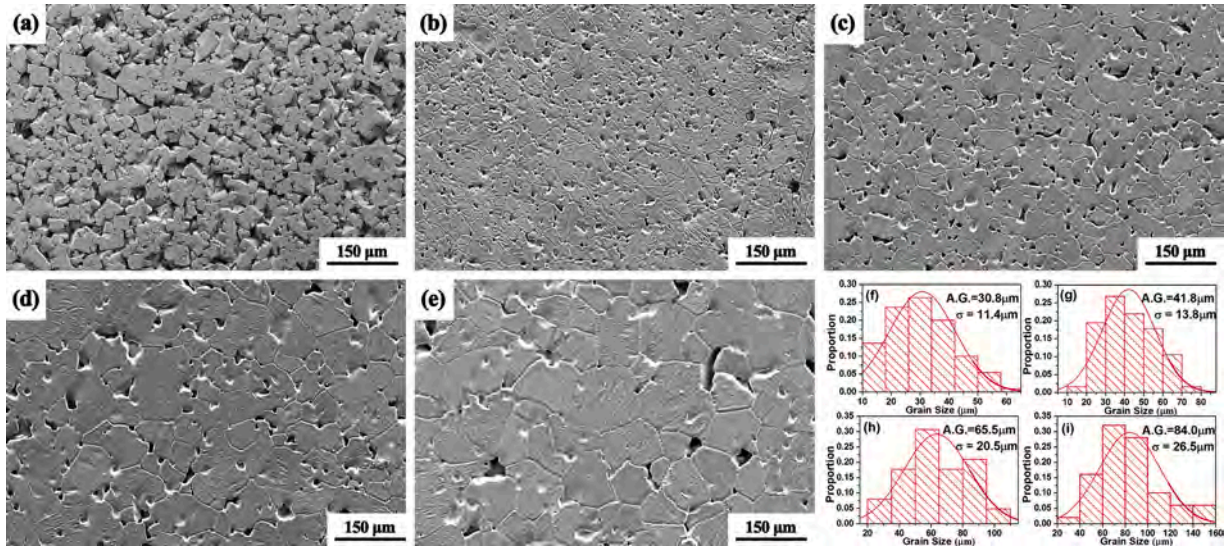


**Fig. 2.** SEM images of the (a) cold sintered and (b-e) post annealed LiF ceramics annealed at 650 °C, 700 °C, 750 °C, and 800 °C, respectively. (f-i) Corresponding grain size distributions, standard deviations ( $\sigma$ ), and average grain sizes (A.G.) of Fig. (b-e).

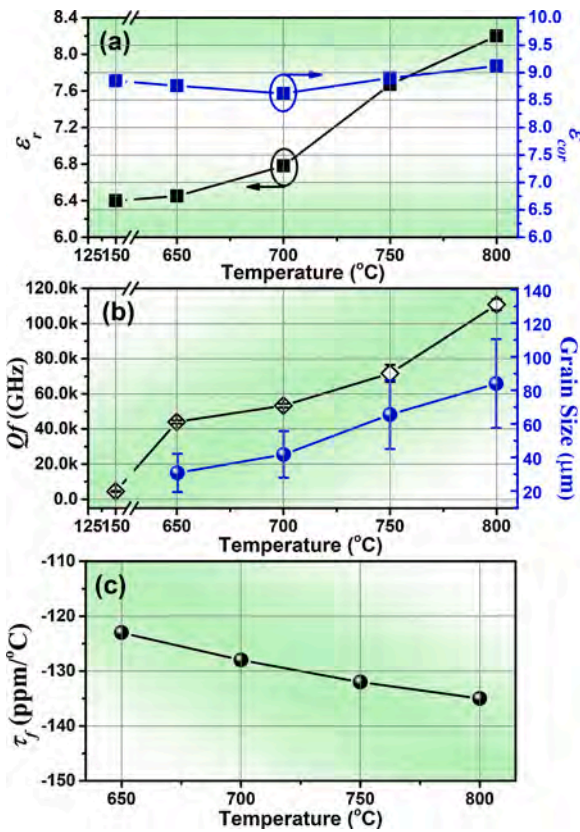


**Fig. 3.** (a)  $\epsilon_r$ ,  $\epsilon_m$ , (b)  $Q_f$  values and the averages grain size, and (c)  $\tau_f$  values of LiF ceramics as functions of processing temperatures.

surfaces of the ceramics. As shown in Fig. 2(a), the microstructure of the as cold-sintered sample consists of cubic-shaped grains, where the grain size and morphology are quite similar with those of LiF raw powder shown in the supporting information, Figure S2. Large open pores can be easily observed, which corresponds to the relatively low density of ~78 %. Upon post-annealing, the grains grow and distinct grain boundaries appear. Fig. 2(f-i) give the grain size distributions and average grain sizes of the post-annealed ceramics. The grain sizes exhibit normal

distributions, and the average grain size increases monotonously with increasing annealing temperature. Some pores however, still exist at the junctions of grains even at the maximum annealing temperature of 800 °C (see Fig. 2(d)). According to Bullard and Lei et al., LiF is harder to densify than oxides as the surface energy of LiF is much lower [12,22]. For example, the (100) surface free energy of LiF (34 μJ/cm<sup>2</sup>) is much lower than that of Al<sub>2</sub>O<sub>3</sub> (90.5 μJ/cm<sup>2</sup>) and MgO (100 μJ/cm<sup>2</sup>), which indicates a smaller driving force of diffusion and grain growth [22]. Since it is difficult to further increase the annealing temperature due to melting, further improvement of the densification may be achieved via modifying the cold sintering process, such as optimizing the amount of solvent or the applied holding pressure.

Fig. 3 shows the MW dielectric properties of the LiF ceramics as function of the processing temperatures.  $\epsilon_r$  of as cold-sintered ceramics is ~6.4 and increases significantly with increasing annealing temperature until a maximum of 8.2 at 800 °C. The trend of  $\epsilon_r$  is in good agreement with the variation of relative density, indicating that the microstructure is the dominating factor in controlling  $\epsilon_r$ . According to Alford et al., the effect of porosity ( $P$ ) on  $\epsilon_r$  is revealed using the following equation: [23]

$$\epsilon_r = \epsilon_{cor} \left( 1 - \frac{3P(\epsilon_{cor} - 1)}{2\epsilon_{cor} + 1} \right) \quad (1)$$

where  $\epsilon_{cor}$  is the porosity corrected dielectric constant, whose values are listed in Table 1 and plotted in Fig. 3(a).  $\epsilon_{cor}$  shows little variation, remaining at ~8.8, which confirms that porosity plays the determining role in the resultant  $\epsilon_r$ .

The low  $Q_f$  values (4487 GHz) of as cold-sintered LiF ceramics are ascribed to the porous microstructure but they improve greatly to a maximum of 110,800 GHz for samples annealed at 800 °C, surpassing reported values via conventional sintering (73,880 GHz). These results indicate that CS and the subsequent annealing are highly beneficial in suppressing dielectric loss [12]. In the absence of phase transitions or impurities, the variation of  $Q_f$  is mainly determined by extrinsic defects such as pores and grain boundaries [24]. Optimization of microstructure is therefore, critical for improving  $Q_f$ . Moreover, as shown in Fig. 3(b), the variation of grain size with annealing temperature adopts a similar trend to that of  $Q_f$ , which further confirms the positive effect of microstructural optimization through enhanced densification. In principle, a defect-free LiF single-crystal should exhibit close to intrinsic dielectric losses (~192,400 GHz), which can be regarded as the upper limit for LiF ceramics [13]. This suggests that further improvement of  $Q_f$  in LiF

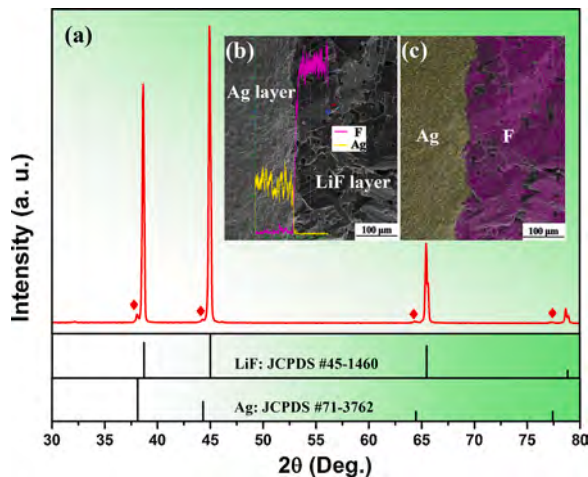


Fig. 4. (a) XRD pattern, (b) SEM image and (c) element mapping result of LiF-Ag composite co-fired at 800 °C for 3 h.

ceramics is still possible via optimization of the microstructure.

$\tau_f$  of as-cold sintered LiF is not evaluated as its resonant response was too faint but for the post-annealed samples, it decreased with increasing temperature, from  $-123 \text{ ppm}/^\circ\text{C}$  to  $-135 \text{ ppm}/^\circ\text{C}$  at 650 °C and 800 °C, respectively.  $\tau_f$  is related to the thermal expansion coefficient ( $\alpha_L$ ) and the temperature dependence of dielectric constant ( $\epsilon_e$ ) via the following equation [25].

$$\tau_f = -\alpha_L - \frac{1}{2}\epsilon_e \quad (3)$$

In this study,  $\alpha_L$  is a constant value, and  $\tau_e$ , and thus  $\tau_f$ , is proportional to  $\epsilon_r$ . Therefore, the variation of  $\tau_f$  is adequately explained as resulting from an increase in  $\epsilon_r$ . In summary, the optimum microwave dielectric properties ( $\epsilon_r = 8.2$ ,  $Qf = 110,800 \text{ GHz}$ ,  $\tau_f = -135 \text{ ppm}/^\circ\text{C}$ ) of LiF ceramics are achieved by pre-densifying using CS and subsequent post-annealing at 800 °C.

To further evaluate the chemical compatibility with metallic electrode, the as cold sintered sample is co-fired with Ag colloids at 800 °C for 3 h and the XRD pattern and SEM image of the LiF-Ag composite are shown in Fig. 4. All diffraction peaks are assigned to LiF and Ag, indicating excellent chemical compatibility. The SEM image presents a discrete boundary between LiF and Ag, which is confirmed from the concentration profiles as functions of distance on both sides of the interface. Moreover, the element mapping result shown in Fig. 4(c) could further confirm the excellent chemical compatibility between LiF and Ag.

#### 4. Conclusions

78 % dense LiF ceramics were prepared via a cold sintering process. Subsequent post-annealing at 650 °C–800 °C led to grain growth and improved the relative density up to 92 %. Optimum microwave dielectric properties ( $\epsilon_r = 8.2$ ,  $Qf = 110,800 \text{ GHz}$ , and  $\tau_f = -135 \text{ ppm}/^\circ\text{C}$ ) were dominated by the ceramic microstructure, and obtained for the densest samples with the largest grain size, post annealed at 800 °C.  $Qf$  values were 1.5 times greater than for conventionally sintered ceramics (78,800 GHz) and were chemically compatible with Ag electrodes, suggesting cold sintered, post annealed LiF may be a promising component in LTCC technology.

#### Declaration of Competing Interest

The authors declare no conflicts of interest.

#### Acknowledgments

Financial supports from the National Natural Science Foundation of China under grant numbers (51802062, 51672063) and Postdoctoral Science Foundation of Zhejiang Province under grant number (ZJ2020008) are greatly appreciated.

#### Appendix A. Supplementary data

Supplementary material related to this article can be found, in the online version, at doi:<https://doi.org/10.1016/j.jeurceramsoc.2020.09.073>.

#### References

- [1] M.T. Sebastian, R. Uric, H. Jantunen, Low-loss dielectric ceramic materials and their properties, *Int. Mater. Rev.* 60 (2015) 392–412.
- [2] T.A. Vanderah, Talking ceramics, *Science* 298 (2002) 1182–1184.
- [3] M.T. Sebastian, H. Jantunen, Low loss dielectric materials for LTCC applications: a review, *Int. Mater. Rev.* 53 (2008) 57–90.
- [4] B. Liu, L. Yi, L. Li, X.M. Chen, Densification and microwave dielectric properties of  $\text{Ca}_{1.15}\text{Sm}_{0.85}\text{Al}_{0.85}\text{Ti}_{0.15}\text{O}_4$  ceramics with  $\text{B}_2\text{O}_3$  addition, *J. Alloys. Compd.* 653 (2015) 351–357.
- [5] B. Liu, L. Yi, X.M. Chen, Effects of  $\text{B}_2\text{O}_3$  addition on sintering behavior and microwave dielectric properties of  $(\text{Sr}_{0.6}\text{Ca}_{0.4})\text{LaAlO}_4$  ceramics, *Mater. Res. Bull.* 67 (2015) 230–233.
- [6] Y. Atsushi, H. Ogawa, A. Kan, H. Ohsato, Y. Higashida, Microwave dielectric properties of  $\text{Mg}_4\text{Nb}_2\text{O}_9$ –3.0wt.% LiF ceramics prepared with  $\text{CaTiO}_3$  additions, *J. Eur. Ceram. Soc.* 25 (2005) 2871–2875.
- [7] Z. Fu, P. Liu, J. Ma, X. Zhao, H. Zhang, Novel series of ultra-low loss microwave dielectric ceramics:  $\text{Li}_2\text{Mg}_3\text{BO}_6$  (B = Ti, Sn, Zr), *J. Eur. Ceram. Soc.* 36 (2016) 625–629.
- [8] C. Li, H. Xiang, M. Xu, Y. Tang, L. Fang,  $\text{Li}_2\text{AgGeO}_4$  (A = Zn, Mg): two novel low-permittivity microwave dielectric ceramics with olivine structure, *J. Eur. Ceram. Soc.* 38 (2018) 1524–1528.
- [9] D. Zhou, C.A. Randall, L. Pang, H. Wang, J. Guo, G. Zhang, X. Wu, L. Shui, X. Yao, Microwave dielectric properties of  $\text{Li}_2\text{WO}_4$  ceramic with ultra-low sintering temperature, *J. Am. Ceram. Soc.* 94 (2011) 348–350.
- [10] K. Wissel, T. Vogel, S. Dasgupta, A.D. Fortes, P.R. Slater, O. Clemens, Topochemical fluorination of  $n = 2$  Ruddlesden-Popper type  $\text{Sr}_3\text{Ti}_2\text{O}_7$  to  $\text{Sr}_3\text{Ti}_2\text{O}_5\text{F}_4$  and its reductive defluorination, *Inorg. Chem.* 59 (2019) 1153–1163.
- [11] Z. Zhang, Y. Tang, H. Xiang, A. Yang, Y. Wang, C. Yin, Y. Tian, L. Fang,  $\text{Li}_5\text{Ti}_2\text{O}_6\text{F}$ : a new low-loss oxyfluoride microwave dielectric ceramic for LTCC applications, *J. Mater. Sci.* 55 (2020) 107–115.
- [12] X. Song, K. Du, J. Li, X. Lan, W. Lu, X. Wang, W. Lei, Low-fired fluoride microwave dielectric ceramics with low dielectric loss, *Ceram. Int.* 45 (2019) 279–286.
- [13] R.G. Geyer, J.B. Jarvis, J. Krupka, Dielectric characterization of single-crystal LiF,  $\text{CaF}_2$ ,  $\text{MgF}_2$ ,  $\text{BaF}_2$ , and  $\text{SrF}_2$  at microwave frequencies, *Proceedings of Annual Report Conference on IEEE Electrical Insulation and Dielectric Phenomena* (2004) 493–497. CEIDP'04, 2004.
- [14] H. Guo, A. Baker, J. Guo, C.A. Randall, Cold sintering process: a novel technique for low-temperature ceramic processing of ferroelectrics, *J. Am. Ceram. Soc.* 99 (2016) 3489–3507.
- [15] D. Wang, B. Siame, S. Zhang, G. Wang, X. Ju, J. Li, Z. Lu, et al., Direct integration of cold sintered, temperature-stable  $\text{Bi}_2\text{Mo}_2\text{O}_9$ – $\text{K}_2\text{MoO}_4$  ceramics on printed circuit boards for satellite navigation antennas, *J. Eur. Ceram. Soc.* 40 (2020) 4029–4034.
- [16] L. Li, H. Yan, W.B. Hong, S.Y. Wu, X.M. Chen, Dense gypsum ceramics prepared by room-temperature cold sintering with greatly improved mechanical properties, *J. Eur. Ceram. Soc.* 40 (2020) 4689–4693.
- [17] W.B. Hong, L. Li, M. Cao, X.M. Chen, Plastic deformation and effects of water in room-temperature cold sintering of NaCl microwave dielectric ceramics, *J. Am. Ceram. Soc.* 101 (2018) 4038–4043.
- [18] W.B. Hong, L. Li, H. Yan, S.Y. Wu, H.S. Yang, X.M. Chen, Room-temperature-densified  $\text{H}_3\text{BO}_3$  microwave dielectric ceramics with ultra-low permittivity and ultra-high  $Qf$  value, *J. Mater.* 6 (2020) 233–239.
- [19] Y. Ji, K. Song, X. Luo, B. Liu, H.B. Baftroei, D. Wang, Microwave dielectric properties of  $(1-x)\text{Li}_2\text{MoO}_4$ – $x\text{Mg}_2\text{SiO}_4$  composite ceramics fabricated by cold sintering process, *Front. Mater.* 6 (2019) 256.
- [20] W.M. Haynes, *CRC Handbook of Chemistry and Physics*, CRS Press, 2017.
- [21] F. Bouville, A.R. Studart, Geologically-inspired strong bulk ceramics made with water at room temperature, *Nat. Commun.* 8 (2017) 14655.
- [22] J.W. Bullard, A.W. Searcy, Microstructural development during sintering of lithium fluoride, *J. Am. Ceram. Soc.* 80 (1997) 2395–2400.
- [23] S.J. Penn, N.M. Alford, A. Templeton, X.R. Wang, M.S. Xu, M. Reece, K. Schrapel, Effects of porosity and grain size on the microwave dielectric properties of sintered alumina, *J. Am. Ceram. Soc.* 80 (1997) 1885–1888.
- [24] B. Liu, Y.H. Huang, K.X. Song, L. Li, X.M. Chen, Structural evolution and microwave dielectric properties in  $\text{Sr}_2(\text{Ti}_{1-x}\text{Sn}_x)\text{O}_4$  ceramics, *J. Eur. Ceram. Soc.* 38 (2018) 3833–3839.
- [25] B. Liu, L. Li, X.Q. Liu, X.M. Chen, Structural evolution of  $\text{SrLaAl}_{1-x}(\text{Zn}_{0.5}\text{Ti}_{0.5})_x\text{O}_4$  ceramics and effects on their microwave dielectric Properties, *J. Mater. Chem. C Mater. Opt. Electron. Devices* 4 (2016) 4684–4691.